

Viologen-Calix[6]arene Pseudorotaxanes. Ion-Pair Recognition and Threading/Dethreading Molecular Motions

Alberto Credi,^{*,†} Stephane Dumas,[†] Serena Silvi,[†] Margherita Venturi,[†] Arturo Arduini,^{*,‡} Andrea Pochini,[‡] and Andrea Secchi[‡]

Dipartimento di Chimica "G. Ciamician", Università degli Studi di Bologna, via Selmi 2, 40126 Bologna, Italy, and Dipartimento di Chimica Organica e Industriale, Università degli Studi di Parma, Parco Area delle Scienze 17/a, 43100 Parma, Italy

alberto.credi@unibo.it

Received April 8, 2004

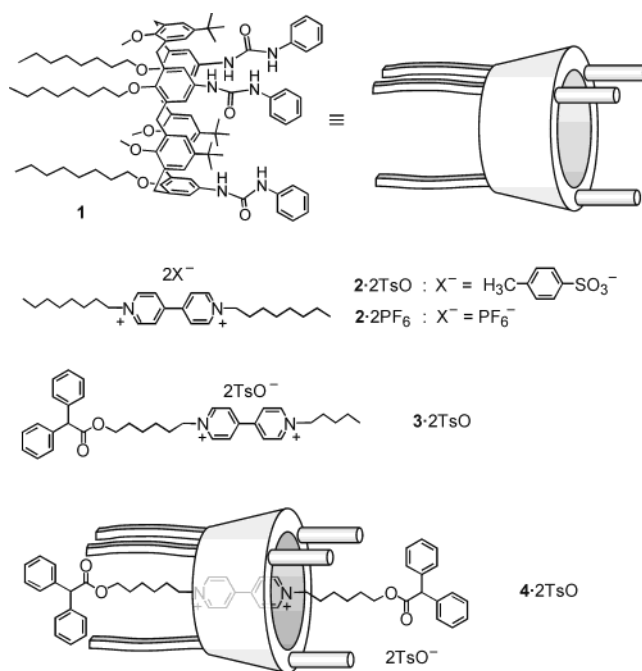
A calix[6]arene wheel, whose cavity has been extended and rigidified by *N*-phenylureido groups on the upper rim, forms pseudorotaxane species with molecular axles containing the viologen (4,4'-bipyridinium) unit in CH₂Cl₂ solution. In these conditions, the self-assembly process is very efficient, with associated ΔG° values of around -8 kcal mol^{-1} . The counteranions of the bipyridinium-based threads play indeed an important role in the formation of the complex. The use of either tosylate or hexafluorophosphate salts of the guests affects both the stability of the complexes and the rate of the threading process. Such effects have been interpreted in terms of ion-pair recognition, suggesting that coordination of the counteranions of the viologen thread by the ureido groups of the calixarene wheel is crucial for the breaking of tight ion pairs prior to threading. The rate constants of the threading/dethreading reactions coupled with the redox processes of the viologen unit of the axle have been obtained by means of cyclic voltammetry. The pseudorotaxane species undergo fast dethreading (submicrosecond time scale) on electrochemical reduction of the guest. The heterogeneous electron-transfer kinetics for the reduction of the viologen unit is slowed upon encapsulation into the calixarene cavity.

Introduction

Threaded and interlocked chemical species¹ have been attracting considerable attention, not only for their structural features but also because of the variety of properties and functions that can be engineered within them. For instance, catenanes and rotaxanes are versatile candidates for constructing molecular devices and machines^{2–5} because they can be designed to perform a variety of functions, including mechanical-like movements, when subjected to an external chemical, photochemical, or electrochemical stimulation.

Calixarenes⁶ are widely used in supramolecular chemistry as versatile platforms for the synthesis of artificial receptors. The binding properties of the calix[6]arene derivative **1** (Chart 1), which is "preorganized" by the presence of 1,3,5-trimethoxy-2,4,6-trioctyloxy groups on

CHART 1. Structural Formulas of the Compounds Examined



the lower rim and bears three phenylureido moieties⁷ as an extension of the cavity, have been exploited⁸ to obtain

(7) For calix[4]arenes with ureido groups in the upper rim, see: Evans, A. J.; Matthews, S. E.; Cowley, A. R.; Beer, P. D. *Dalton Trans.* **2003**, 4644.

[†] Università di Bologna.

[‡] Università di Parma.

(1) *Molecular Catenanes, Rotaxanes and Knots*; Sauvage, J.-P., Dietrich-Buchecker, C. O., Eds.; Wiley-VCH: Weinheim, 1999.

(2) Balzani, V.; Credi, A.; Venturi, M. *Molecular Devices and Machines—A Journey into the Nano World*; Wiley-VCH: Weinheim, 2003.

(3) *Acc. Chem. Res.* **2001**, *34* (6), 409–522 (Special Issue on Molecular Machines; Stoddart, J. F., Ed.).

(4) *Struct. Bond.* **2001**, *99*, 1–281 (Special Volume on Molecular Machines and Motors; Sauvage, J.-P., Ed.).

(5) Balzani, V.; Credi, A.; Raymo, F. M.; Stoddart, J. F. *Angew. Chem., Int. Ed.* **2000**, *39*, 3348.

(6) (a) *Calixarenes in Action*; Mandolini, L., Ungaro, R., Eds.; Imperial College Press: London, 2000. (b) *Calixarenes 2001*; Asfari, Z., Böhmer, V., Harrowfield, J., Vicens, J., Eds.; Kluwer: Dordrecht, 2001.

the first examples of pseudorotaxane and rotaxane species having a calixarene as the wheel component. More recently, it has been demonstrated⁹ that the different structural and chemical information present on the two distinct rims of the calixarene can govern the direction of the axle threading process, giving rise to "oriented" pseudorotaxanes. 1,1'-Dialkyl-4,4'-bipyridinium thread-like compounds such as those shown in Chart 1 have been selected as the axle components, owing to the interesting and well-known¹⁰ physicochemical properties of the 4,4'-bipyridinium (viologen) unit.

One of the distinctive features of these novel pseudorotaxanes is the fact that the calixarene host is potentially capable of complexing the counteranions¹¹ of the bipyridinium guest through hydrogen-bonding interactions with the NH ureido groups. Such an anion complexation has been clearly evidenced by X-ray crystallography in the solid state⁸ and by ¹H NMR spectroscopy in solution⁹ for the pseudorotaxane formed between **1** and 1,1'-dioctyl-4,4'-bipyridinium diiodide. It can be expected that the counteranions of the dicationic guest play an important role in the formation of the pseudorotaxane, from both a thermodynamic and a kinetic viewpoint, for the following reasons: (i) in the apolar solvents employed for the self-assembly process, the bipyridinium species can form tight ion pairs with their anions, and (ii) the size and binding properties of the wheel cavity are suitable for the inclusion of only the dicationic portion of the axle. Therefore, it is reasonable to assume that separation of the dicationic thread from its counteranions has to take place before insertion into the cavity of the calixarene wheel. The simultaneous recognition of cations and anions^{12,13} is crucial to achieve an efficient threading process in low-polarity solvents^{14,15} and can provide an additional means for controlling self-assembly.¹⁶

Pseudorotaxanes in which the threading/dethreading of the axle and wheel components can be controlled by appropriate stimuli constitute basic prototypes of molecular machines.¹⁷ It can be anticipated⁵ that the valuable redox properties of the viologen unit incorporated in the molecular threads can be exploited to trigger the assembly/disassembly of the corresponding pseudorotaxanes. It should be noted, however, that despite the large

(8) Arduini, A.; Ferdani, R.; Pochini, A.; Secchi, A.; Uguzzoli, F. *Angew. Chem., Int. Ed.* **2000**, *39*, 3453.

(9) Arduini, A.; Calzavacca, F.; Pochini, A.; Secchi, A. *Chem. Eur. J.* **2003**, *9*, 793.

(10) Monk, P. M. S. *The Viologens: Physicochemical Properties, Synthesis and Applications of the Salts of 4,4'-Bipyridine*; Wiley: New York, 1998.

(11) For recent reviews on anion recognition, see: (a) Snowden, T. S.; Anslyn, E. V. *Curr. Opin. Chem. Biol.* **1999**, *3*, 740. (b) Beer, P. D.; Gale, P. A. *Angew. Chem., Int. Ed.* **2001**, *40*, 486. (c) Amendola, V.; Fabbri, L.; Mangano, C.; Pallavicini, P.; Poggi, A.; Taglietti, A. *Coord. Chem. Rev.* **2001**, *219*, 821.

(12) For reviews on ion-pair recognition, see: (a) Reetz, M. T. In *Comprehensive Supramolecular Chemistry*; Atwood, J. L., Davies, J. E. D., Macnicol, D. D., Vögtle, F., Eds.; Pergamon Press: Oxford, 1996; Vol. 2, p 553. (b) Gale, P. A. *Coord. Chem. Rev.* **2003**, *240*, 191.

(13) For recent examples of ion-pair recognition, see: (a) Shivanyuk, A.; Rebek, J., Jr. *Proc. Natl. Acad. Sci. U.S.A.* **2001**, *98*, 7662. (b) Arduini, A.; Giorgi, G.; Pochini, A.; Secchi, A.; Uguzzoli, F. *J. Org. Chem.* **2001**, *66*, 8302. (c) Arduini, A.; Brindani, E.; Giorgi, G.; Pochini, A.; Secchi, A. *J. Org. Chem.* **2002**, *67*, 6188. (d) Jones, J. W.; Zakharov, L. N.; Rheingold, A. L.; Gibson, H. W. *J. Am. Chem. Soc.* **2002**, *124*, 13378. (e) Rekharsky, M.; Inoue, Y.; Tobey, S.; Metzger, A.; Anslyn, E. V. *J. Am. Chem. Soc.* **2002**, *124*, 14959. (f) de Silva, A. P.; McClean, G. D.; Pagliari, S. *Chem. Commun.* **2003**, 2010. (g) Shivanyuk, A.; Friese, J. C.; Rebek, J., Jr. *Tetrahedron* **2003**, *59*, 7067. (h) Tobey, S. L.; Anslyn, E. V. *J. Am. Chem. Soc.* **2003**, *125*, 10963.

TABLE 1. Absorption and Luminescence Data (CH₂Cl₂, rt)

compound	absorption		luminescence	
	λ_{\max} (nm)	ϵ (M ⁻¹ cm ⁻¹)	λ_{\max} (nm)	Φ
1	250 ^a	60 000 ^a	340	2.5×10^{-3}
2 ·2TsO	270	24 000	<i>b</i>	<i>b</i>
2 ·2PF ₆	265	15 000	350	9×10^{-3}
3 ·2TsO	270	25 000	<i>b</i>	<i>b</i>
4 ·2TsO	259	88 000	<i>b</i>	<i>b</i>
	440 ^a	750 ^a		

^a Shoulder on the lower energy side of an intense band. ^b Not luminescent.

number of reports on similar systems,²⁻⁵ little is known about the dynamics of the threading and dethreading processes in solution.

Here we report the results of a photophysical investigation, including stopped-flow absorption spectroscopy, on the self-assembly of the tris(*N*-phenylureido)calix[6]arene **1** with the molecular threads **2**²⁺ (as its tosylate and hexafluorophosphate salts) and **3**²⁺ (as its tosylate salt) in CH₂Cl₂ solution (Chart 1).^{18,19} We have also studied the threading/dethreading processes of **1** with **2**·2PF₆ by cyclic voltammetry and addressed the effect of wheel encapsulation on the heterogeneous electron-transfer kinetics of the redox-active unit contained in the axle by comparison with the model rotaxane **4**²⁺ (as its tosylate salt).

Results and Discussion

Absorption and Luminescence Spectra. The absorption and luminescence data for the examined compounds in CH₂Cl₂ at room temperature are gathered in Table 1.

The calix[6]arene **1** exhibits (Figure 1) a strong absorption tail in the near-UV region, extending down to ca. 310 nm, and a very weak fluorescence band with λ_{\max} = 340 nm. Such a luminescence band can be safely assigned to electronic transitions of the phenylureido units by comparison with the behavior of the model compound *N,N'*-diphenylurea.

The threadlike species **2**·2TsO, **2**·2PF₆, and **3**·2TsO show the typical¹⁰ $\pi\pi^*$ absorption band of the viologen unit, with maximum at ca. 270 nm. The absorption bands of **2**·2TsO and **3**·2TsO are nearly identical and exhibit

(14) The self-assembly of a pseudorotaxane promoted by anion recognition has been recently reported; see: Wisner, J. A.; Beer, P. D.; Berry, N. G.; Tomapatanaget, B. *Proc. Natl. Acad. Sci. U.S.A.* **2002**, *99*, 4983.

(15) For a detailed quantitative treatment of the effect of ion pairing on the stability of pseudorotaxanes with cationic axles, see: (a) Jones, J. W.; Gibson, H. W. *J. Am. Chem. Soc.* **2003**, *125*, 7001. (b) Huang, F.; Jones, J. W.; Slobodnik, C.; Gibson, H. W. *J. Am. Chem. Soc.* **2003**, *125*, 14458.

(16) The ion pairing between a cationic threadlike compound and chloride ions in CH₂Cl₂ has been exploited to dethread the corresponding pseudorotaxane. Montalti, M.; Prodi, L. *Chem. Commun.* **1998**, 1461.

(17) Pioneering work: Ballardini, R.; Balzani, V.; Gandolfi, M. T.; Prodi, L.; Venturi, M.; Philp, D.; Ricketts, H. G.; Stoddart, J. F. *Angew. Chem., Int. Ed. Engl.* **1993**, *32*, 1301.

(18) Hexafluorophosphate and *p*-toluenesulfonate (tosylate) ions have been selected as prototypical examples of "innocent" and complexing anions, respectively. Other dioctyl viologen salts in our hands (dichloride and dibromide) could not be used because of their very poor solubility in CH₂Cl₂.

(19) *Supramolecular Chemistry of Anions*; Bianchi, A., Bowman-James, K., Garcia-España, E., Eds.; Wiley-VCH: New York, 1997.

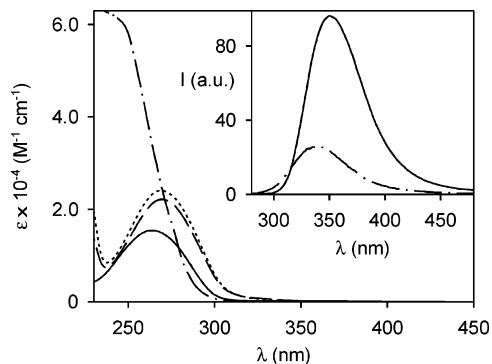


FIGURE 1. Absorption spectra of **1** (· · · ·), **2**·**2PF**₆ (—), **2**·**2TsO** (---) and **3**·**2TsO** (· · · ·). Inset: fluorescence spectra of **1** (· · · ·; $\lambda_{\text{ex}} = 250$ nm) and **2**·**2PF**₆ (—; $\lambda_{\text{ex}} = 265$ nm). Conditions: CH_2Cl_2 , rt.

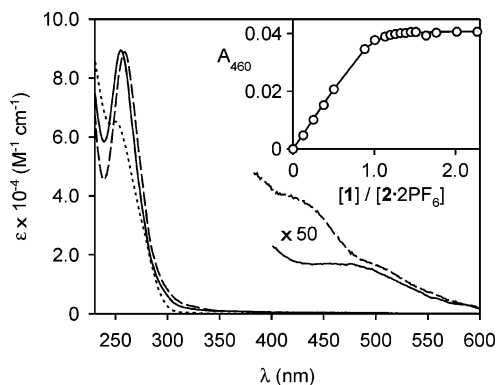


FIGURE 2. Absorption spectra (CH_2Cl_2 solution, 293 K) of the pseudorotaxane **1** (· · · ·) **2**·**2PF**₆ (—), compared to the sum of the spectra of the separated components (· · · ·). The dashed line represents the absorption spectrum of the rotaxane **4**·**2TsO**. Inset: absorption changes at 460 nm upon addition of **1** to a 1.2×10^{-4} M solution of **2**·**2PF**₆.

higher λ_{max} and ϵ values compared to the band of **2**·**2PF**₆. The latter compound shows a weak fluorescence band²⁰ with $\lambda_{\text{max}} = 350$ nm, whereas the tosylate salts of **2**²⁺ and **3**²⁺ are not luminescent. Such a behavior suggests that these species are present in CH_2Cl_2 solution as tight ion pairs (vide infra)^{15b,21,22} and that the viologen moiety of **2**²⁺ and **3**²⁺ undergoes electronic interactions with the tosylate counteranions. More specifically, the quenching of the luminescence band of the viologen unit in the TsO⁻ salts can be attributed to a photoinduced process within the ion pairs.²³

The absorption spectra of 1:1 mixtures of **1** and threads **2**·**2TsO**, **2**·**2PF**₆, or **3**·**2TsO** differ from the sum of the spectra of the separated species and are similar to the spectrum of rotaxane **4**·**2TsO** (Figure 2). Besides changes in the UV absorption bands of the molecular components, a new broad and weak absorption band with λ_{max} around

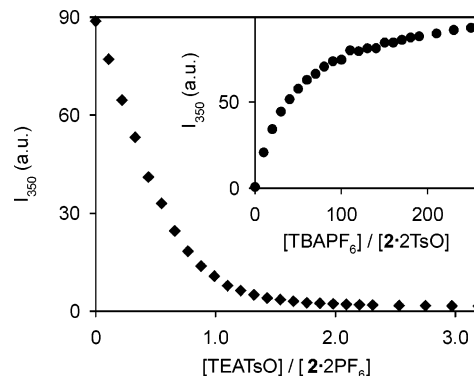


FIGURE 3. Changes in the fluorescence intensity at 350 nm of a 1.2×10^{-4} M solution of **2**·**2PF**₆ upon addition of TEATsO and of a 7.6×10^{-5} M solution of **2**·**2TsO** upon addition of TBAPF₆ (inset). Conditions: CH_2Cl_2 , 293 K, $\lambda_{\text{ex}} = 280$ nm.

460 nm shows up in the absorption spectra of the mixtures. The fluorescence bands typical of **1** and **2**·**2PF**₆ can no longer be seen²³ when these two species are mixed in an equimolar ratio. All of these observations are consistent with the formation of a complex between **1** and the threads **2**²⁺ or **3**²⁺. The pseudorotaxane nature of such complexes has been confirmed^{8,9} by ¹H NMR spectroscopy in solution and, in the case of the iodide salt of **2**²⁺, by X-ray crystallography in the solid state. The supramolecular structure is stabilized by a variety of interactions, including π -electron donor/acceptor and C–H $\cdots\pi$ interactions, C–H \cdots O hydrogen bonds, and hydrogen bonding between the counteranions of the guest and the ureidic NH fragments of the host. The visible absorption band observed for the pseudorotaxanes is attributed to the charge-transfer interactions between the aromatic rings of **1** and the bipyridinium unit of **2**²⁺ or **3**²⁺. These interactions are also responsible for the quenching of the fluorescence bands of **1** and **2**·**2PF**₆, since they introduce new excited states that offer a radiationless deactivation path to the upper lying, potentially luminescent levels.⁵

It is interesting to note that, although the absorption spectra of **2**·**2TsO** and **2**·**2PF**₆ are noticeably different, the spectra of their 1:1 mixtures with **1** are similar but not identical. Such an observation indicates that the counteranions can no longer interact closely with **2**²⁺ once it is threaded into **1** and are indeed part of the complex, in agreement with the structural data^{8,9} and in keeping with the fact that the cavity of **1** can accommodate only a viologen dication.

Spectrophotometric Titrations. The absorption and luminescence spectral changes observed in titration experiments have been employed to probe the ion pairing between **2**²⁺ and either tosylate or hexafluorophosphate anions and to investigate the formation of the pseudorotaxanes.

The addition of tetraethylammonium tosylate (TEA-TsO) to a 1.2×10^{-4} M solution of **2**·**2PF**₆ causes changes in the UV absorption band of the viologen unit and the quenching²³ of the fluorescence band with $\lambda_{\text{max}} = 350$ nm (Figure 3). On the other hand, the addition of tetrabutylammonium hexafluorophosphate (TBAPF₆)²⁴ to a 7.6

(20) Peon, J.; Tan, X.; Hoerner, D.; Xia, C.; Luk, Y. F.; Kohler, B. *J. Phys. Chem. A* **2001**, *105*, 5768.

(21) Schneider, H.-J. *Angew. Chem., Int. Ed. Engl.* **1991**, *30*, 1417. (b) Price, E. In *The Chemistry of Nonaqueous Solvents*; Lagowski, J. J., Ed.; Academic Press: New York, 1966; Vol. 1, p 67.

(22) Bipyridinium dications are known to aggregate in nonpolar solvents. From the absorption spectra, we have found no evidence of aggregation in the concentration range employed.

(23) Because of the very short lifetime ($\tau < 1$ ns) of the luminescence bands of both **1** and **2**·**2PF**₆, the occurrence of dynamic quenching can be ruled out in our experimental conditions.

(24) The same results were obtained by using TEAPF₆ in the place of TBAPF₆, indicating the innocence of the tetraalkylammonium cations in such ion-pairing processes.

TABLE 2. Apparent Stability Constants (K_{st1}) and Threading (k_1) and Dethreading (k_{-1}) Rate Constants for Examined Pseudorotaxanes (CH_2Cl_2 , 293 K)

complex	K_{st1} (10^6 M^{-1}) ^a	k_1 ($10^3 \text{ M}^{-1} \text{ s}^{-1}$)	k_{-1} (s^{-1}) ^b
1 ⊃ 2 · 2 TsO	6 ± 3	1700 ± 300	0.3 ± 0.2
1 ⊃ 2 · 2 PF ₆	0.8 ± 0.5	6 ± 1	0.008 ± 0.006
1 ⊃ 3 · 2 TsO	3 ± 1	58 000 ± 1000	19 ± 7

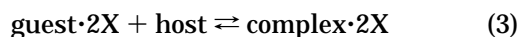
^a Calculated according to the equation $K_{st1} = [\text{complex}]/[\text{host}][\text{guest}\cdot 2\text{X}]$, using $[\text{host}] = [\text{host}]^0 - [\text{complex}]$ and $[\text{guest}\cdot 2\text{X}] = [\text{guest}\cdot 2\text{X}]^0 - [\text{complex}]$. ^b $k_{-1} = k_1/K_{st1}$.

$\times 10^{-5} \text{ M}$ solution of **2**·**2**TsO causes absorption spectral changes opposite to those observed in the previous experiment and the appearance of the fluorescence band typical of **2**·**2**PF₆ (Figure 3, inset). The addition of TEATsO to a solution of **2**·**2**TsO does not produce absorption and luminescence spectral changes, whereas the addition of TBAPF₆ to a $3.4 \times 10^{-6} \text{ M}$ solution of **2**·**2**PF₆ causes a small increase of the luminescence band with $\lambda_{\text{max}} = 350 \text{ nm}$ until a plateau is reached after addition of ca. 10 equiv.

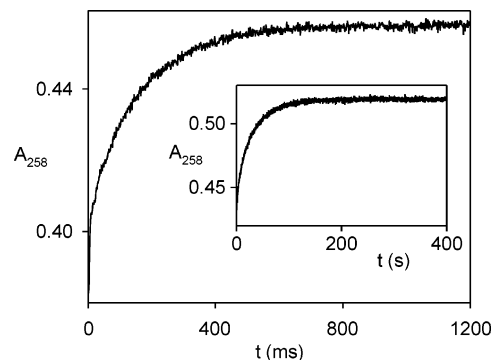
These observations clearly indicate that **2**·**2**TsO and **2**·**2**PF₆ exist as tight ion pairs^{15b} in our experimental conditions and that the electrostatic interaction²⁵ of **2**²⁺ with TsO⁻ anions is stronger than that with PF₆⁻ ions, as could be expected on the basis of the electronic properties of tosylate and hexafluorophosphate anions.¹⁹

The values for the apparent stability constant of the pseudorotaxanes **1**⊃**2**·**2**TsO, **1**⊃**2**·**2**PF₆, and **1**⊃**3**·**2**TsO in CH_2Cl_2 at 293 K are reported in Table 2. The absorption changes at 460 nm upon addition of **1** to a solution of **2**·**2**PF₆ are shown in the inset of Figure 2.

Because the anions are intrinsic to the system in all of the experiments described here, there is always an interplay between the pairing of the dicationic thread with its counteranions (eq 1) and the self-assembly of the pseudorotaxane.^{14–16,26} Two limiting cases can be identified in this regard, that is, the active species for the assembly of the complex is either the unpaired guest (eq 2) or the ion pair between the guest and its anions (eq 3). In the first case, of course, ion pairing is in competition with the self-assembly equilibrium and occurs at the expense of pseudorotaxane formation.^{15,16} The large values found for the apparent stability constants, considering the extensive cation/anion association observed in our conditions, indicate that the ion pairs of the thread species play indeed an active role in the self-assembly of the pseudorotaxane.



The fact that the pseudorotaxane formed between **1** and **2**·**2**TsO is more stable than that between **1** and **2**·**2**PF₆, despite the higher ion-pairing ability of TsO⁻ compared to PF₆⁻ ions, implies that the anions are in fact

**FIGURE 4.** Absorption changes at 258 nm upon rapid mixing of equimolar amounts of **1** and **2**·**2**TsO or **2**·**2**PF₆ (inset) in CH_2Cl_2 at 293 K. Notice the different time scale of the two diagrams. The concentration of the reactants after mixing was $5.0 \times 10^{-6} \text{ M}$.

component parts of the complex and contribute to its stabilization.^{12–15} Such results are in agreement with NMR and crystallographic studies, which reveal that the anions are hydrogen-bonded to the ureidic groups of **1**, and with the fact that tosylate ions are much better hydrogen bond acceptors than hexafluorophosphate ions. It is worthwhile recalling that an opposite effect related to ion pairing, that is, the stronger the guest ion pairs, the weaker the binding by the host, has been observed^{15,25,27} in systems where the host cannot provide specific stabilization for the counteranion of the cationic guest.

Stopped-Flow Absorption Experiments. The rate of the self-assembly process of the pseudorotaxanes, that is, the threading of the axles **2**²⁺ and **3**²⁺ into the cavity of **1**, has been measured by stopped-flow experiments, carried out by monitoring the absorption changes upon rapid mixing of the calixarene wheel with the axle. In all cases, the data could be interpreted satisfactorily with a kinetic model for a 1:1 association equilibrium, giving second-order threading rate constants. These values are gathered in Table 2, together with those of the corresponding first-order dethreading rate constants.²⁸ Figure 4 shows the absorption changes at 258 nm upon rapid mixing of equimolar amounts of **1** and **2**·**2**TsO or **2**·**2**PF₆ (inset) in CH_2Cl_2 at 293 K.

It can be noticed that the values for the threading and dethreading rate constants are largely dependent on the nature of the counteranion of the **2**²⁺ thread. The use of tosylate in the place of hexafluorophosphate anions causes the increase of both the threading and the dethreading rate constants by more than 2 orders of magnitude (Table 2). In fact, the threading process in the case of **2**·**2**PF₆ is quite slow; it takes place on a time scale of minutes in our experimental conditions (Figure 4, inset).

To explain these differences, it is useful to recall that the tight ion pairs of the guest species must dissociate prior to threading of the dicationic axle into the wheel, and the counteranions can be complexed by the ureidic

(25) (a) Bartoli, S.; Roelens, S. *J. Am. Chem. Soc.* **1999**, *121*, 11908. (b) Bartoli, S.; Roelens, S. *J. Am. Chem. Soc.* **2002**, *124*, 8307.

(26) For a detailed study on the role of the counteranion in the formation of complexes involving cationic species, see: Hunter, C. A.; Low, C. M. R.; Rotger, C.; Vinter, J. G.; Zonta, C. *Chem. Commun.* **2003**, 834.

(27) (a) Arnecke, R.; Böhmer, V.; Cacciapaglia, R.; Dalla Cort, A.; Mandolini, L. *Tetrahedron* **1997**, *53*, 4901. (b) Böhmer, V.; Dalla Cort, A.; Mandolini, L. *J. Org. Chem.* **2001**, *66*, 1900.

(28) Pseudorotaxanes made of the cyclobis(paraquat-*p*-phenylene) macrocycle and naphthalene-based molecular threads exhibit much faster kinetics in acetonitrile or water solution. Venturi, M.; Dumas, S.; Balzani, V.; Cao, J.; Stoddart, J. F. *New J. Chem.* ASAP.

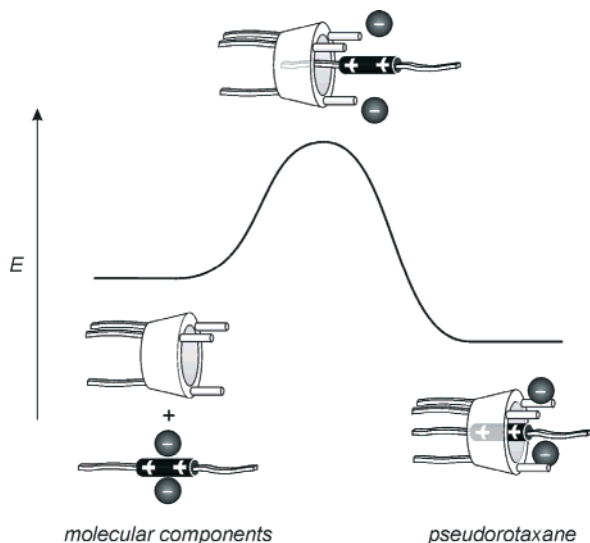


FIGURE 5. Schematic illustration of the free energy change associated with the threading of a viologen dicationic axle into calixarene **1**. The black spheres represent the counteranions of the guest.

units at the upper rim of the calixarene. The threading process could be interpreted by assuming that the “active” species is the unpaired bipyridinium compound and that the threading mechanism involves (i) the dissociation of the ion pair and (ii) subsequent insertion of the unpaired thread species into the calixarene. If the threading rate were determined by the rate of dissociation of the ion pairs of the guest, which is obviously anion-dependent, one would expect a first-order kinetic behavior for the threading process, with no influence by the concentration of the host. This picture is in contrast with our experimental observations. Moreover, we have found that in our conditions the exchange between PF_6^- and TsO^- ions in the ion pair with 2^{2+} is quite fast (below the time resolution of our stopped-flow equipment; see Experimental Section). On the other hand, if the rate-determining step were the insertion of the unpaired thread species into the wheel, the nature of the counteranion of the guest should have no effect on the threading rate.

The present results are not sufficient to assess the detailed mechanism of threading, which is beyond the scope of this work; however, our observations indicate that the separation of the guest ion pairs, the threading of the guest, and the binding of the anions by the ureidic groups of the calixarene occur in a concerted manner. It is therefore reasonable to assume the involvement of a transition state in which the counteranions of the axle are being “disengaged” from the ion pair and “parked” at the upper rim of the wheel (Figure 5). Because the nature of the counteranions of the guest has a large influence on the kinetics but affects only slightly the thermodynamics of formation of the pseudorotaxane, we can conclude that the relative contribution of hydrogen bonds involving the anions and the ureidic groups of the calixarene to the total stabilization energy is substantially higher in the transition state compared to the final threaded structure. This picture is consistent with a transition-state structure like that schematized in Figure 5, in which the bipyridinium unit of the axle is not included in the cavity of the calixarene, and therefore

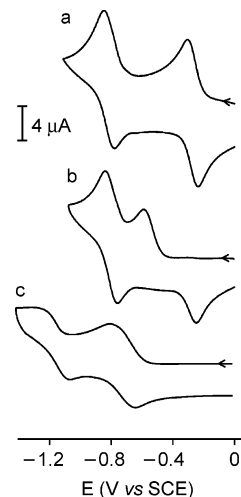


FIGURE 6. Cyclic voltammograms (2×10^{-4} M CH_2Cl_2 solution, 0.05 M TBAPF₆, 293 K; scan rate 0.2 V s^{-1}) for the first and second reduction of the viologen unit in (a) $2 \cdot 2\text{PF}_6$, (b) the pseudorotaxane $1 \supset 2 \cdot 2\text{PF}_6$, and (c) the rotaxane $4 \cdot 2\text{PF}_6$.

the axle-wheel interactions are not effective. Tosylate anions, owing to their higher hydrogen-bonding ability, presumably give a more stable transition state compared to hexafluorophosphate ions, thus accelerating the threading/dethreading process.

The stoppered thread $3 \cdot 2\text{TsO}$ undergoes much faster threading and dethreading compared to $2 \cdot 2\text{TsO}$. On statistical grounds, one would have expected slower kinetics for $3 \cdot 2\text{TsO}$ because it can enter the wheel **1** from only one of its ends. It has recently been observed for other pseudorotaxane systems that the shorter the side chains of the thread, the faster the threading/dethreading process.²⁸ Thus, the behavior observed for $1 \supset 3 \cdot 2\text{TsO}$ is probably related to the fact that the unstoppered alkyl side chain of 3^{2+} , consisting of five carbon atoms, is shorter than the side chains of 2^{2+} , which are made of eight carbon atoms. An alternative, less likely explanation would be that the diphenylacetic ester stopper facilitates the threading/dethreading by stabilizing the transition state.

Cyclic Voltammetry. All of the molecular components examined are electroactive in the potential window examined (from -1.8 to $+1.8 \text{ V vs SCE}$). It should be noted that electrochemical experiments are carried out in the presence of a large excess of TBAPF₆, used as supporting electrolyte. Therefore, the axle species are present in solution as ion pairs with the PF_6^- anions, irrespective of the salt employed.

Calixarene **1** shows several irreversible oxidation processes, most likely attributable to its oxybenzene units, that will not be discussed and no reduction process. The axles $2 \cdot 2\text{PF}_6$ and $3 \cdot 2\text{PF}_6$ exhibit (Figure 6a) two mono-electronic and reversible reduction processes ($E_{1/2}' = -0.29 \text{ V}$, $E_{1/2}'' = -0.81 \text{ V vs SCE}$), characteristic¹⁰ of the viologen unit, and no oxidation process.

The inclusion of either 2^{2+} or 3^{2+} into the cavity of **1** causes a large negative shift of the first reduction potential of the viologen unit of the axle (Figure 6b). In other words, the axle becomes more difficult to reduce, reflecting the stabilization offered by the wheel. The same behavior is found for the first reduction of the rotaxane

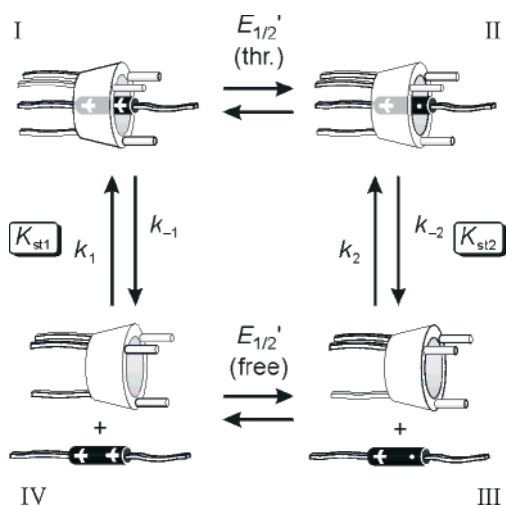


FIGURE 7. Square scheme mechanism for the one-electron reduction of $1\supset 2\cdot 2\text{PF}_6$. I and III represent the stable states, whereas II and IV are metastable intermediates. The counteranions have been omitted for clarity.

$4\cdot 2\text{PF}_6$ ($E_{1/2}' = -0.74$ V; Figure 6c). The second reduction process of the $1\supset 2\cdot 2\text{PF}_6$ and $1\supset 3\cdot 2\text{PF}_6$ systems occurs at the same potential as for the free axle (Figure 6ab), whereas it is shifted to more negative values in the rotaxane $4\cdot 2\text{PF}_6$ ($E_{1/2}'' = -1.18$ V; Figure 6c). These results show that one-electron reduction of 2^{2+} or 3^{2+} promotes its dethreading from **1**, in line with the behavior of several related bipyridinium-containing pseudorotaxanes^{2–5,17,29,30} and in keeping with the fact that one-electron reduction decreases the π -electron acceptor and H-bonding donor abilities of the viologen unit, thereby destabilizing the pseudorotaxane structure.

From Figure 6b it can be noticed that the first reduction process of $1\supset 2\cdot 2\text{PF}_6$ is characterized by a very large separation between the cathodic and anodic peaks. Such a voltammetric pattern is indicative of kinetic complications, not unexpected for systems in which redox processes can cause structural rearrangements.^{29,31} The behavior observed, which can be discussed on the basis of a square scheme (Figure 7), has been elucidated by detailed cyclic voltammetric experiments. In particular, the presence of an anodic peak at ca. -0.26 V, assigned to reoxidation of the previously decomplexed 2^{2+} radical cation, suggests that the threading of 2^{2+} into **1** is slow on the voltammetric time scale. Moreover, a second scan performed without the renewal of the diffusion layer (not shown) reveals the presence of a cathodic peak at ca. -0.33 V that becomes more evident as the scan rate is increased. Such a peak is assigned to the reduction of free 2^{2+} originated in the previous scan. This finding indicates that the (re)threading of 2^{2+} into **1** can indeed

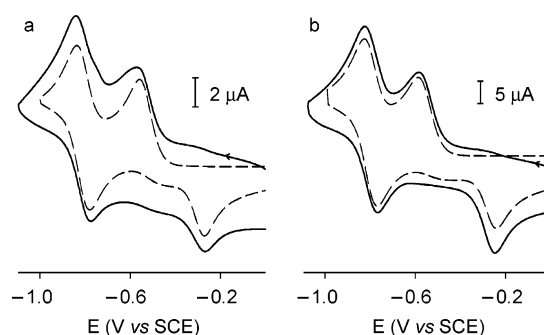


FIGURE 8. Experimental (—) and simulated (---) cyclic voltammograms for the $1\supset 2\cdot 2\text{PF}_6$ system at a scan rate of (a) 50 and (b) 500 mV s^{-1} (2×10^{-4} M CH_2Cl_2 solution, 0.05 M TBAPF_6 , 293 K). The simulated voltammograms have been obtained by using the parameters indicated in the text.

be observed in the time frame of the voltammetric scan, in good agreement with the results of the stopped-flow absorption experiments. The values of the threading rate constant and the stability constant of the pseudorotaxane were employed in digital simulations of the experimental voltammetric curves according to the mechanism of Figure 7. By optimizing the fitting of the simulated voltammograms to the experimental ones for a range of scan rates (Figure 8), the following values for the parameters shown in Figure 7 have been obtained: $E_{1/2}'(\text{free}) = -0.27$ V, $E_{1/2}'(\text{threaded}) = -0.70$ V, $k_2 = 1 \times 10^5 \text{ M}^{-1} \text{ s}^{-1}$, $k_{-2} = 2 \times 10^6 \text{ s}^{-1}$. Therefore, the dethreading of the monoreduced axle 2^{2+} from the wheel occurs in the submicrosecond time scale.

The results of the digital simulations show that direct reduction of the inclusion complex takes place and that the heterogeneous electron-transfer rate constant of the $2^{2+}/2^{2+}$ couple decreases when 2^{2+} is threaded into **1** [$k_{\text{et}}'(\text{threaded}) \approx 0.18 \text{ cm s}^{-1}$].³² Although it is well-known³³ that the inclusion of a redox-active species into a receptor can slow its heterogeneous electron-transfer processes, this effect has rarely been observed³⁰ in pseudorotaxanes and rotaxanes, most likely because the molecular architecture of these compounds does not afford complete encapsulation. Apparently, the extended walls of **1** are capable of shielding efficiently the bipyridinium unit from the electrode surface. This effect has been confirmed by the cyclic voltammetric behavior of the rotaxane $4\cdot 2\text{PF}_6$, in which long-range rearrangements of the axle relative to the wheel are prevented. The heterogeneous electron-transfer rate constant for the first reduction of $4\cdot 2\text{PF}_6$ has been estimated to be $6 \times 10^{-3} \text{ cm s}^{-1}$.

Conclusion

In CH_2Cl_2 the calix[6]arene **1** and the viologen-containing threadlike molecules 2^{2+} and 3^{2+} self-assemble very efficiently to give a pseudorotaxane. We have found that the counteranions of the guest species play an important role in the formation of the complexes. The use of either hexafluorophosphate or tosylate salts for the dicationic

(29) Kim, H.-J.; Jeon, W. S.; Ko, Y. H.; Kim, K. *Proc. Natl. Acad. Sci. U.S.A.* **2002**, *99*, 5007.

(30) Córdova, E.; Bissell, R. A.; Kaifer, A. E. *J. Org. Chem.* **1995**, *60*, 1033.

(31) (a) Cárdenas, D. J.; Livoreil, A.; Sauvage, J.-P. *J. Am. Chem. Soc.* **1996**, *118*, 11980. (b) Mirzoian, A.; Kaifer, A. E. *Chem. Eur. J.* **1997**, *3*, 1052. (c) Ashton, P. R.; Ballardini, R.; Balzani, V.; Baxter, I.; Credi, A.; Fyfe, M. C. T.; Gandolfi, M. T.; Gómez-López, M.; Martínez-Díaz, M.-V.; Piersanti, A.; Spencer, N.; Stoddart, J. F.; Venturi, M.; White, A. J. P.; Williams, D. J. *J. Am. Chem. Soc.* **1998**, *120*, 11932. (d) Amendola, V.; Fabbrizzi, L.; Gianelli, L.; Maggi, C.; Mangano, C.; Pallavicini, P.; Zema, M. *Inorg. Chem.* **2001**, *40*, 3579.

(32) Most bipyridinium dication/radical cation couples exhibit extremely fast heterogeneous electron-transfer kinetics. See ref 10.

(33) Cardona, C. M.; Mendoza, S.; Kaifer, A. E. *Chem. Soc. Rev.* **2000**, *29*, 37.

thread species has an influence on the thermodynamic stability of the pseudorotaxanes and affects markedly the threading/dethreading kinetics. These findings open new interesting perspectives, related to the use of the anions for (i) adding new functionalities to these supramolecular architectures (photo- and electroactive anions could be employed) and (ii) controlling the dynamics of the threading/dethreading processes.

The examined pseudorotaxanes can be disassembled in a fast and reversible manner by one-electron reduction of their axle components. We have also found that the heterogeneous electron-transfer kinetics for the reduction of the bipyridinium unit is slowed upon encapsulation into the calixarene cavity.

These investigations show that ion pairing, an issue that is often overlooked, is of extreme importance, from both a thermodynamic and a kinetic viewpoint, when considering complexation processes in low polarity solvents. Our results provide an insight into the dynamics of self-assembly/induced-disassembly processes of pseudorotaxanes in solution. A further motif of interest, in the light of recent evidence⁹ of directional axle threading in this type of compounds, is related to the design and construction of novel molecular machines exhibiting *unidirectional* threading/dethreading motions.

Experimental Section

Synthesis. Compound **1** was synthesized according to literature procedures. The syntheses of compounds **1**,³⁴ **2**·2TsO⁸, and **3**·2TsO⁹ have already been reported. Compound **2**·2PF₆ was obtained from the corresponding diiodide salt,⁸ by anion exchange with AgPF₆ in methanol/water.

3·2C₇H₇SO₃³⁺ as tosylate salt was obtained from the corresponding dibromide salt, synthesized according to ref 9, by anion exchange with silver tosylate in acetone/water as pink solid: Mp 115–118 °C; ¹H NMR (C₆D₆, 300 MHz) δ 9.4 (br, var, 6H), 8.21 (d, 4H, *J* = 7.5 Hz), 8.1–7.7 (m, 12H), 7.63 (s, 6H), 7.5–7.4 (m, 10H), 7.35 (d, 2H, *J* = 7.4 Hz), 7.2–7.1 (m, 20H), 6.96 (d, 4H, *J* = 7.5 Hz), 6.65 (bt, 5H), 5.20 (s, 1H), 5.18 (s, 1H), 4.55 (bd, 6H), 4.40 (bt, 2H), 4.09 (bt, 2H), 4.0–3.8 (m, 17H), 3.6 (bs, 6H), 3.5–3.4 (m, 14H), 2.01 (s, 6H), 1.74 (s, 27H), 1.7–1.1, 1.0, 0.7 and 0.5 (m, 3bs, 25H); MS (ESI, CH₃OH) *m/z* 1106.0 [M²⁺ – H⁺]⁺.

Absorption and Luminescence Spectra. Measurements were carried out at room temperature (ca. 295 K) on air-equilibrated CH₂Cl₂ (Merck Uvasol) solutions in the concentration range from 5 × 10⁻⁵ to 2 × 10⁻⁴ M. UV-vis absorption and luminescence spectra were recorded with a Perkin-Elmer λ40 spectrophotometer and a Spex Fluorolog τ3 spectrofluorimeter, respectively. For the luminescence spectra, excitation was performed at the wavelength of the absorption maximum. Equipment and procedures for the determination of luminescence quantum yields and lifetimes were reported previously.^{31c} The apparent stability constants of the pseudorotaxanes (Table 2) were calculated by fitting the absorption titration curves according to the equation $K_{st1} = [\text{complex}]/([\text{host}][\text{guest} \cdot 2X])$, using $[\text{host}] = [\text{host}]^0 - [\text{complex}]$ and $[\text{guest} \cdot 2X] = [\text{guest} \cdot 2X]^0 - [\text{complex}]$. The so-obtained values did not change in the range of concentrations examined.

Stopped-Flow Absorption Experiments. Reaction kinetic profiles were collected on air-equilibrated CH₂Cl₂ (Merck Uvasol) solutions at 293 K with an Applied Photophysics SX

18 MV stopped-flow spectrophotometer interfaced to a computer for data collection and analysis. The optical path length of the cell was 1 cm, and the driving ram for the mixing system was operated at the recommended N₂ pressure of 8.5 bar. Under these conditions, the time required to fill the 1-cm observation cell was experimentally determined to be <1.3 ms (based on a test reaction). The concentration of the reactants after mixing was in the range from 5 × 10⁻⁶ to 1 × 10⁻⁵ M. The kinetic absorbance curves were analyzed with a kinetic treatment for an equilibrium A + B ⇌ C as implemented into the SPECFIT software.³⁵ A fitting of the data trace with a simple second-order rate equation, however, was equally satisfactory, owing to the very high value of the equilibrium constant.

Electrochemical Measurements. Cyclic voltammetric (CV) experiments were carried out in argon-purged CH₂Cl₂ (Romil Hi-Dry) with an Autolab 30 multipurpose instrument interfaced to a PC. The working electrode was a glassy carbon electrode (Amel; 0.07 cm²); its surface was routinely polished with a 0.3 μm alumina–water slurry on a felt surface, immediately prior to use. In all cases, the counter electrode was a Pt wire, separated from the solution by a frit; an Ag wire was employed as a quasi-reference electrode, and ferrocene was present as an internal standard. The concentration of the compounds examined was 2 × 10⁻⁴ M; tetrabutylammonium hexafluorophosphate 0.05 M was added as supporting electrolyte. Cyclic voltammograms were obtained at sweep rates varying from 0.02 to 5 V s⁻¹. The IR compensation implemented within the Autolab 30 was used, and every effort was made throughout the experiments to minimize the resistance of the solution. In any instance, the full electrochemical reversibility of the voltammetric wave of ferrocene was taken as an indicator of the absence of uncompensated resistance effects. Digital simulations of the experimental CVs for the **1**⊃**2**·2PF₆ system were obtained on the basis of the square scheme mechanism illustrated in Figure 7 by using the software package DigiSim 3.05.³⁶ The values of *K*₁ (obtained from absorption titrations) and *k*₁ (measured with stopped-flow spectroscopic experiments) were fixed in the simulation, while the values found for the first reduction of **2**·2PF₆ and **4**·2PF₆ were used as initial estimates for *E*_{1/2}'(free) and *E*_{1/2}'(threaded), respectively. The second reduction wave, which always showed electrochemical reversibility in the experimental conditions used, could also be simulated, by extending the mechanism of Figure 6 to the **2**⁺⁰ redox couple. A value of 1 cm s⁻¹, representative of a reversible process under our conditions,³⁷ was employed in the simulation for *k*_{et}'(free) and *k*_{et}'(free). The charge-transfer coefficients were taken as 0.5 in all cases. For the rotaxane **4**·2PF₆, the value of the heterogeneous electron-transfer rate constant was first estimated from the variation in the peak-to-peak separation as a function of the scan rate by using the Nicholson method.³⁸ Such values were then employed in the digital simulations of the cyclic voltammograms by DigiSim.

Acknowledgment. This research was supported by the EU (RTN Project HPRN-CT-2000-00029 “Molecular-Level Devices and Machines”), MIUR (Supramolecular Devices Project), FIRB (Manipolazione molecolare per macchine nanometriche), and the University of Bologna (Funds for Selected Topics).

JO0494127

(35) Binstead, R. A. *SPECFIT*; Spectrum Software Associates: Chapel Hill, NC, 1996.

(36) *DigiSim 3.05*; BioAnalytical Systems: West Lafayette, IN; www.bioanalytical.com.

(37) Bard, A. J.; Faulkner, L. R. *Electrochemical Methods. Fundamentals and Applications*; Wiley: New York, 1980. Chapter 6.

(38) Nicholson, R. S. *Anal. Chem.* **1965**, *37*, 1351.

(34) González, J. J.; Ferdani, R.; Albertini, E.; Blasco, J. M.; Arduini, A.; Pochini, A.; Prados, P.; de Mendoza, J. *Chem. Eur. J.* **2000**, *6*, 73.